Supplement of Earth Syst. Sci. Data, 17, 1515–1528, 2025
https://doi.org/10.5194/essd-17-1515-2025-supplement

Supplement of

An in situ daily dataset for benchmarking temporal variability of groundwater recharge

Pragnaditya Malakar et al.

Correspondence to: Pragnaditya Malakar (pragnadityamalakar@gmail.com) and Mukesh Kumar (mkumar4@eng.ua.edu)

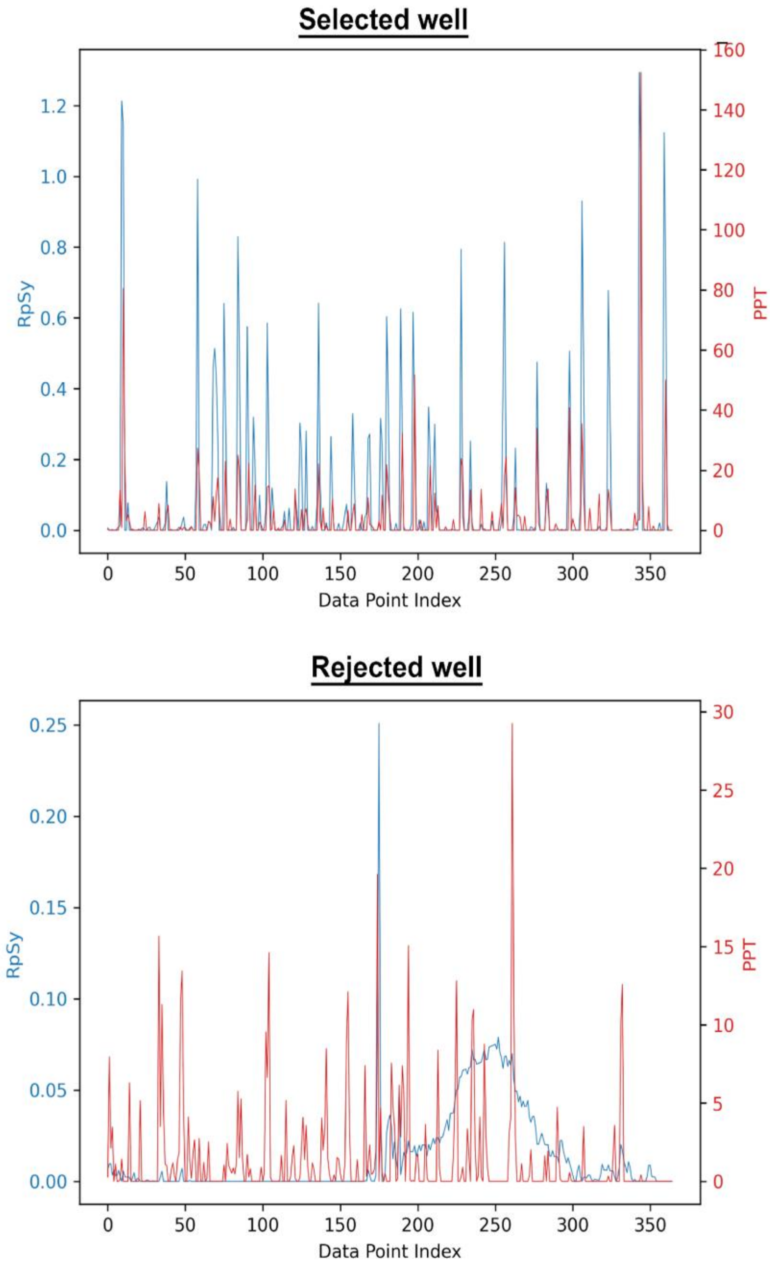

Figure S1: The hydrographs (a) and (b) show precipitation (Ppt) in mm, and estimated recharge per unit specific yield (RpSy, discussed later) in m per day, for a selected and a rejected well, respectively. The selection/rejection is implemented based on the maximum lag correlation threshold, which ensures that the well is more likely to experience event based GWR response to precipitation signals.

Supplementary text S1: Comparison of the nearest stream and groundwater level

Jasechko et al. (2021) compared the elevations of the groundwater level and a constant stream level at bank full height. This study uses a similar approach by identifying the nearest streams to individual wells using high-resolution National Hydrography Dataset Plus Version 2 (McKay et al., 2012). Groundwater well and stream bank elevations are extracted using a 10m resolution 3DEP digital elevation model (DEM) (U.S. Geological Survey, 2019), along with groundwater level time series and bank full-depth estimates (Wieczorek et al., 2019). The elevation difference between groundwater and river levels (E_{diff}) is calculated as follows.

$$E_{diff} = E_{GWL} - med(Depth_{GWL}) - E_{Stream} + BFH_{stream} \quad \text{(S1)}$$

Here E_{GWL} and E_{Stream} denote groundwater level and river level elevation which are extracted from the DEM. The terms $med(Depth_{GWL})$ and BFH_{stream} represent the median of depth to groundwater level observations and bank full height of stream respectively. Eq. (S1) assumes that the elevations extracted using DEM correspond to the elevation of the bank. Since NHD data represents a high-resolution stream network, this assumption is valid due to the likelihood of DEM resolutions being coarser than stream widths. The locations of the wells, distances to nearest streams, differences in elevations, bank full depth and bank full-width estimates are plotted in Figure S2 and S3. Streams with negative E_{diff} values can be classified as losing or influent streams, but this classification also depends on the distance to the nearest well. When the distance is large, the influent flux from stream to well may be negligible. Another important factor is bank full width; this study assumes that rivers with a bank full width of less than 5m are narrow enough to not significantly contribute to groundwater recharge. Considering these criteria, the number of wells used for benchmarking can be narrowed down, as given in Table S1 and Figure S2, S3.

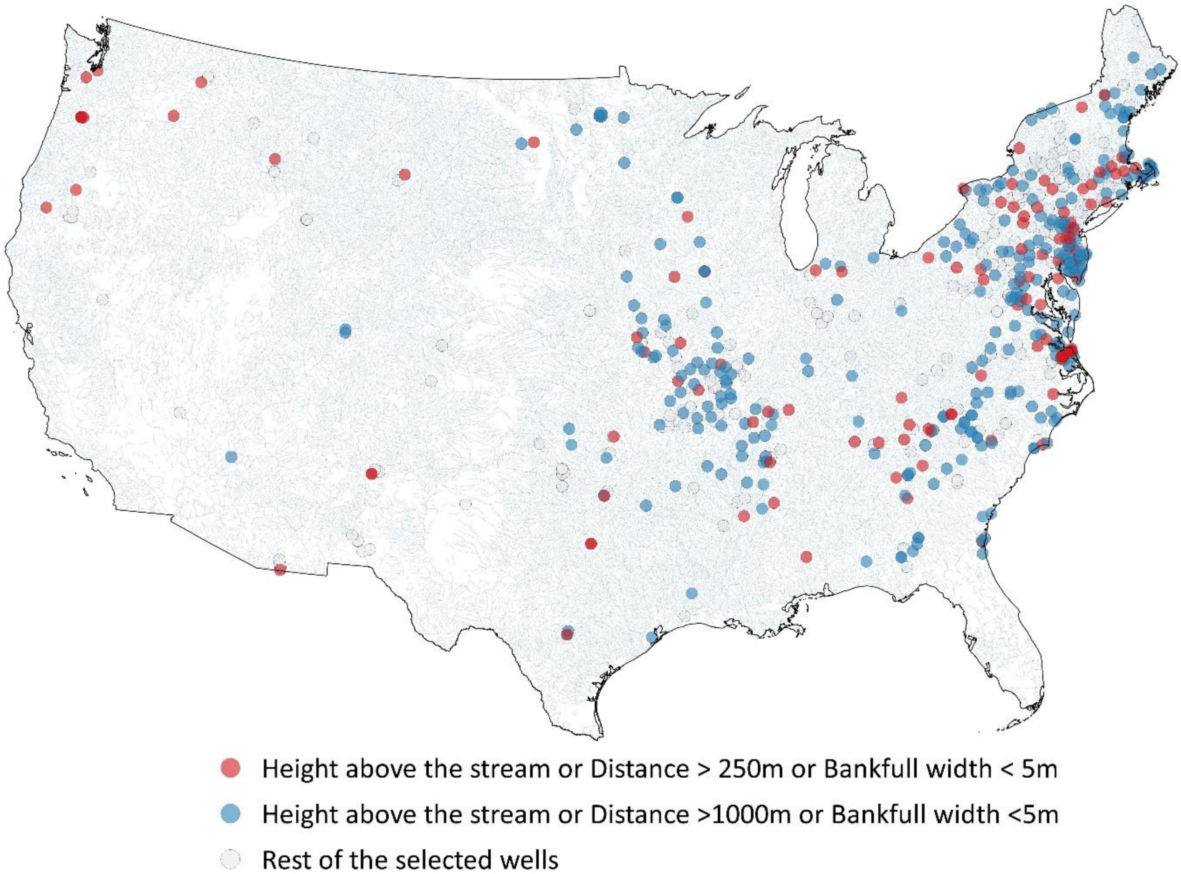

Figure S2: The number of wells selected based on different criteria, which includes distance the nearest stream (shown using blue lines).

Table S1: The number of wells selected based on different criteria of the nearest stream

Condition of selection of wells	No. of stations
Height above the stream or Distance >250m	388
Height above the stream or Distance >1000m	304
Height above the stream or Distance >250m or Bankfull width <5m	420
Height above the stream or Distance >1000m or Bankfull width <5m	380

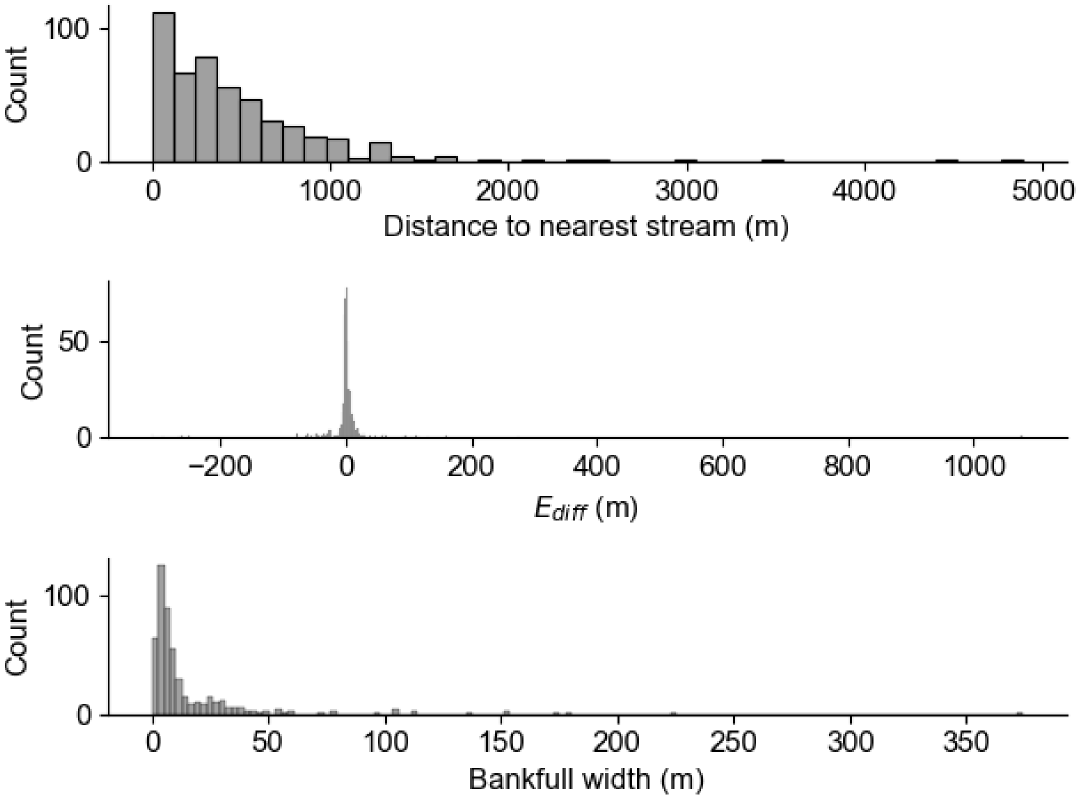

Figure S3: Number of wells with respect to distance to the nearest stream, E_{diff} and bank full width (in meters)

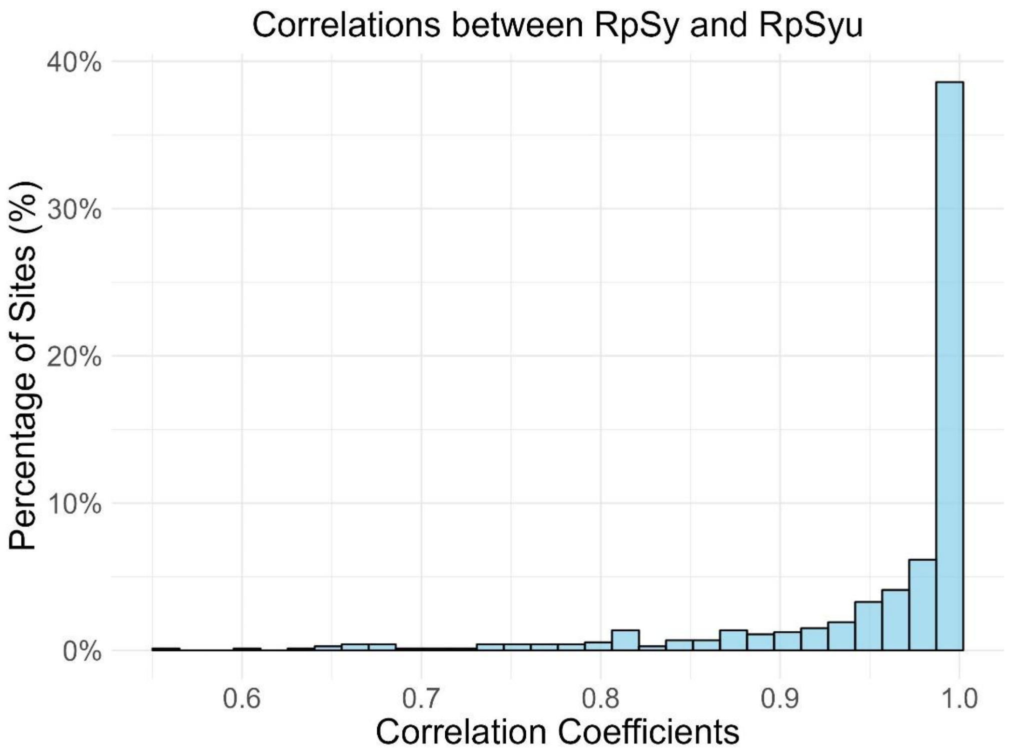

Figure S4: Correlations between RpSy and RpSyu.

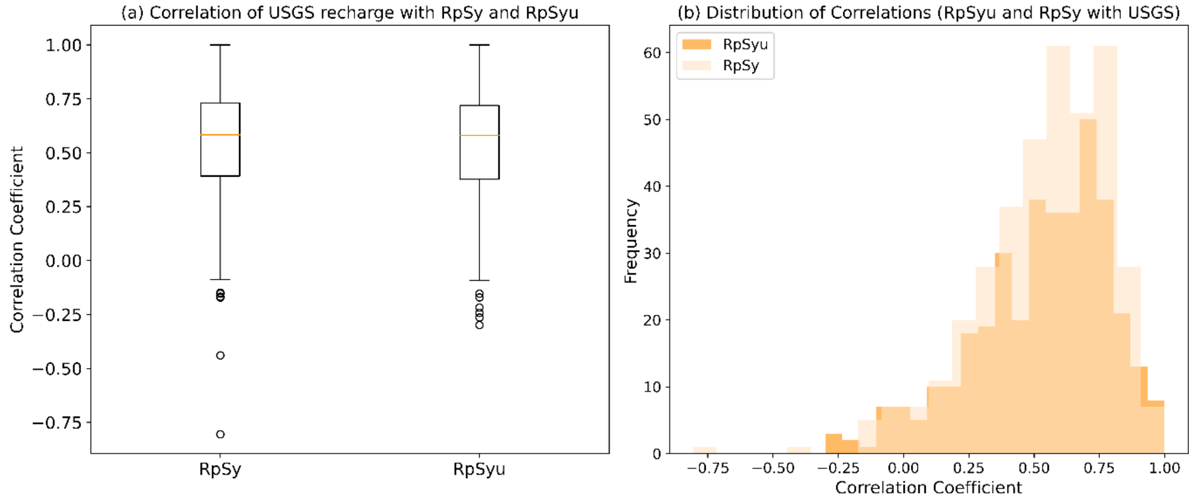

Figure S5: Comparison of RpSy and RpSyu correlations with USGS recharge data. (a) correlation spread for both RpSy and RpSyu, with the orange line indicating the median correlation; (b) histograms show the correlation distributions for RpSy and RpSyu with USGS recharge.

Table S2: Summary Statistics for Correlation between RpSyu, RpSy and USGS recharge.

	Correlation_RpSyu	Correlation_RpSy
mean	0.531049	0.541389
standard deviation	0.256786	0.251975
minimum	-0.29906	-0.8052
5% (first quartile)	0.376744	0.391686
50% (median or second quartile)	0.58046	0.582712
75% (third quartile)	0.719417	0.730783
maximum	0.999441	0.999503

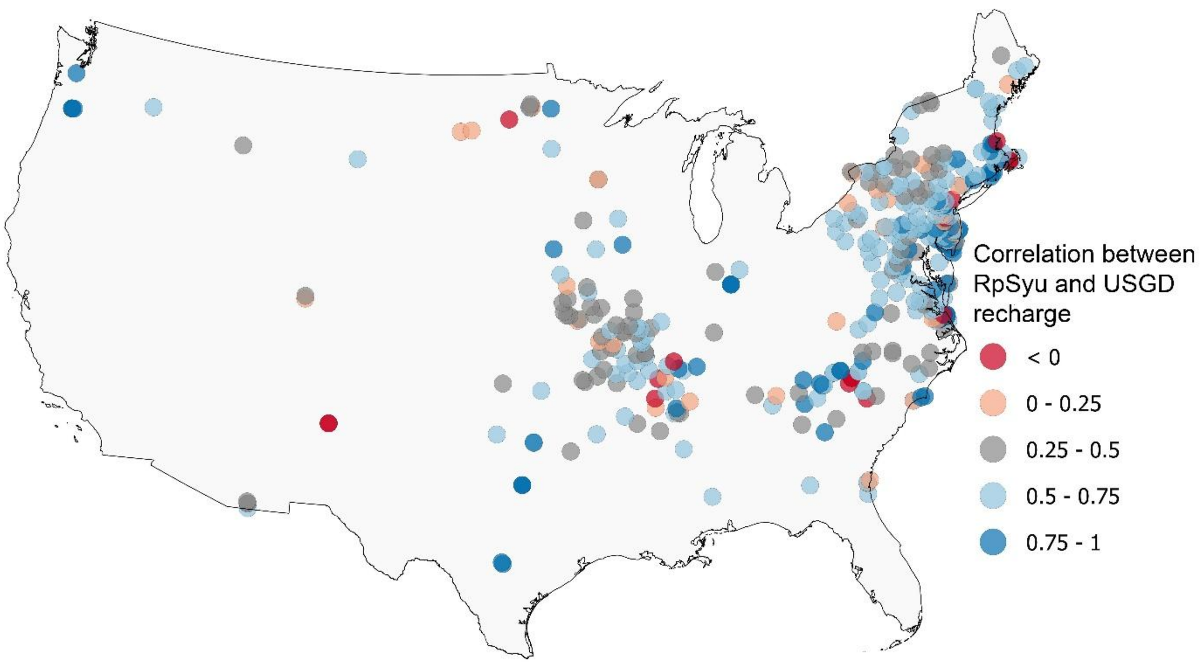

Figure S6: Spatial variation of temporal correlation between RpSyu and USGS recharge.

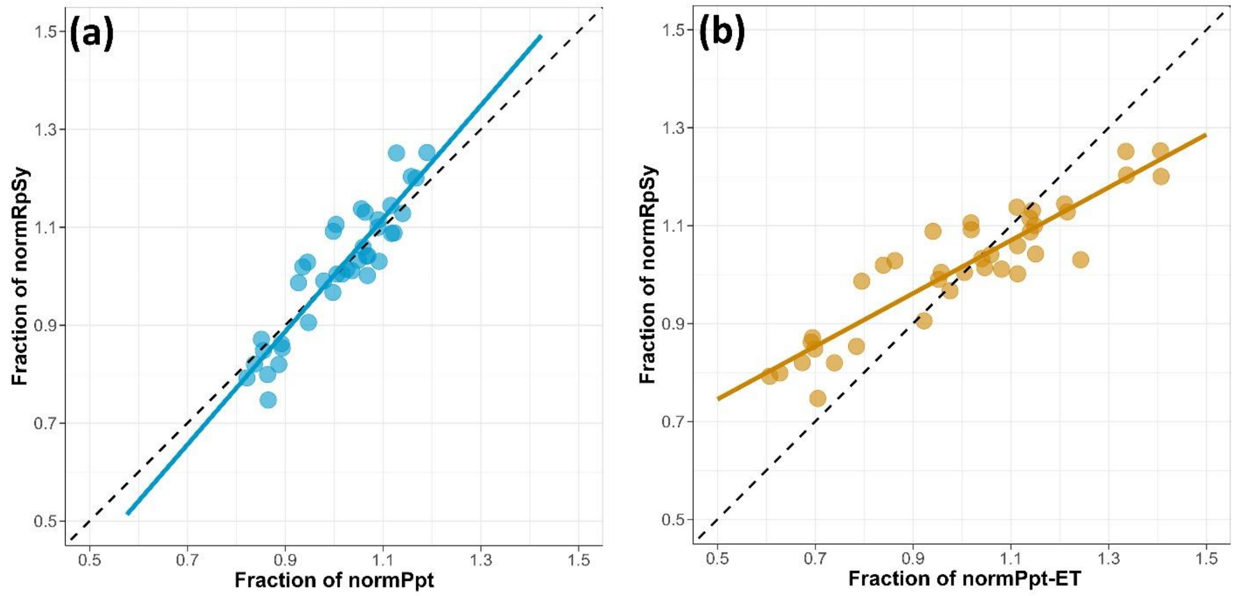

Figure S7: Scatter plot showing the Inter-annual variation between (a) normalized annual recharge (normRpSy) and precipitation (normPpt) shown using blue dots; (b) normalized annual recharge (normRpSy) and Ppt-ET (normPpt-ET) shown using orange dots. The scatter of normRpSy vs normPpt has a higher slope relative to the 1:1 line. The scatter of normRpSy vs normPpt-ET has a lower slope relative to the 1:1 line.

Table S3. Inter-annual variation of normalized annual recharge (normRpSy), precipitation (normPpt), and Ppt-ET (normPpt-ET).

Year	RpSy	RpSyu	Ppt	Ppt-ET	R^2 for Rpsy	R^2 for Rpsyu
1983	103.0	103.1	109.2	124.3	**RpSy Vs. Ppt**	**RpSyu Vs. Ppt**
1984	125.2	92.9	112.8	133.5	0.839	0.029
1985	79.9	108.4	86.4	62.8	**RpSy Vs. Ppt-ET**	**RpSyu Vs. Ppt-ET**
1986	84.8	103.4	85.5	69.9	0.837	0.026
1987	101.1	106.8	103.6	108.1		
1988	79.2	107.8	82.2	60.7		
1989	104.2	98.6	106.9	115.1		
1990	102.9	106.5	94.6	86.3		
1991	105.9	117.0	106.0	111.4		
1992	90.6	102.7	94.8	92.2		
1993	109.2	80.8	99.8	101.9		
1994	113.1	94.9	106.3	114.4		
1995	87.1	102.9	85.1	69.4		
1996	120.3	89.4	115.8	133.7		
1997	110.6	120.6	100.4	101.9		
1998	113.8	106.8	105.6	111.2		
1999	82.0	99.9	88.7	73.9		
2000	85.3	104.0	89.4	78.4		
2001	82.0	114.9	83.7	67.4		

2002	74.7	98.2	86.5	70.5	
2003	120.0	118.5	116.7	140.7	
2004	114.4	109.0	111.6	121.0	
2005	101.9	110.7	93.6	83.9	
2006	104.1	86.3	106.7	105.9	
2007	98.7	89.4	92.7	79.5	
2008	100.2	85.3	106.8	111.4	
2009	100.4	111.6	100.6	100.5	
2010	111.5	113.4	109.0	113.9	
2011	112.8	87.9	114.0	121.5	
2012	86.2	110.2	89.2	69.2	
2013	101.4	90.3	102.6	104.7	
2014	99.0	99.0	97.9	95.2	
2015	96.7	99.5	99.7	97.6	
2016	103.3	84.4	104.9	104.1	

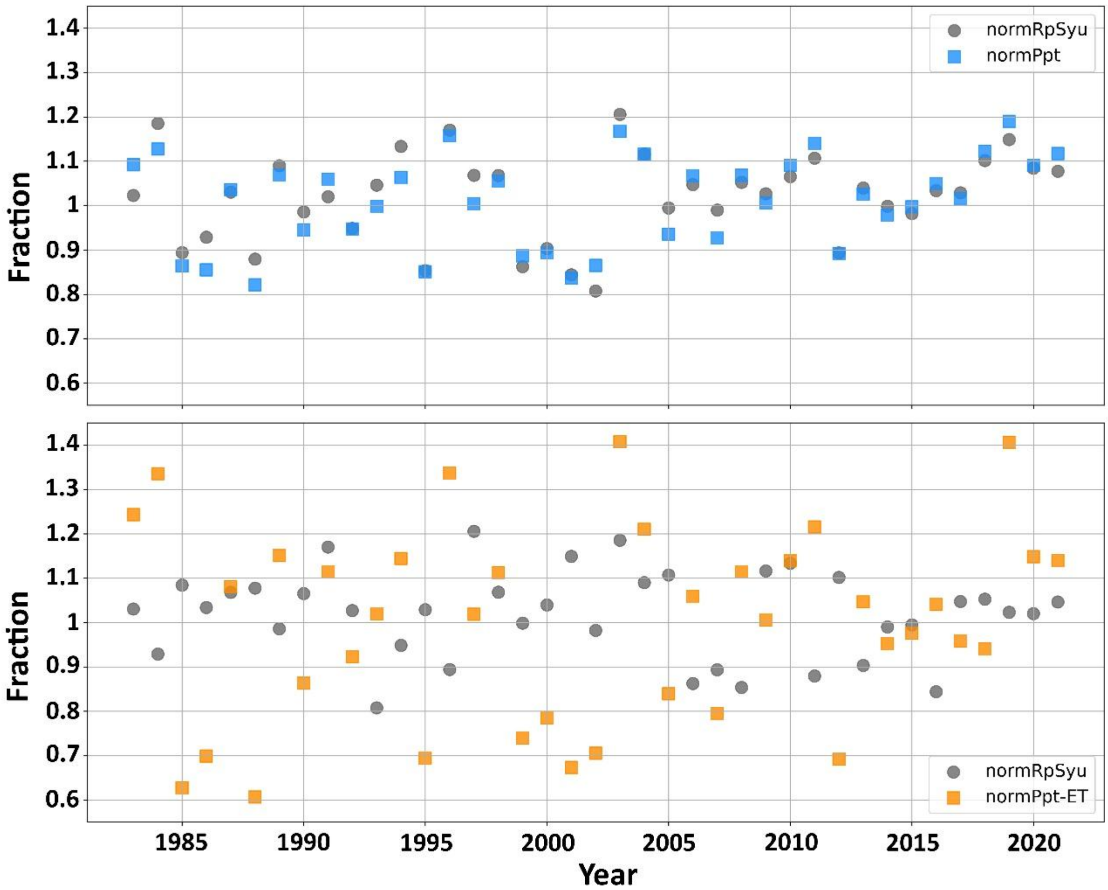

Figure S8: Inter-annual variation of normalized annual recharge (normRpSyu, shown using grey solid dots), precipitation (normPpt, blue squares), and Ppt-ET (normPpt-ET, orange squares).

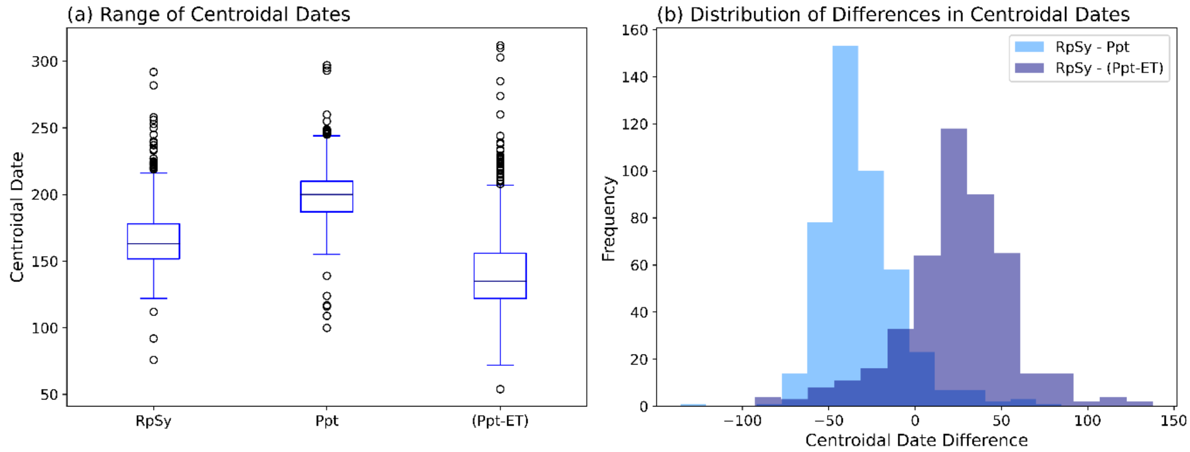

Figure S9: Variation of RpSy centroidal dates in comparison with Precipitation (Ppt) and Precipitation Minus Evapotranspiration (Ppt-ET) centroids for 485 locations. (a) the distribution of centroidal dates for RpSy, Ppt, and Ppt-ET; (b) Histogram of Centroidal Date Differences.

RpSy data files for each wells

Date	RpSy (m)	RpSyu (m)
$mm_1/dd_1/yyyy_1$	$rpsy_{111}$	$rpsyu_{111}$
$mm_1/dd_2/yyyy_1$	$rpsy_{121}$	$rpsyu_{121}$
$mm_1/dd_3/yyyy_1$	$rpsy_{131}$	$rpsyu_{131}$
$mm_1/dd_4/yyyy_1$	$rpsy_{141}$	$rpsyu_{141}$
$mm_1/dd_5/yyyy_1$	$rpsy_{151}$	$rpsyu_{151}$
$mm_1/dd_6/yyyy_1$	$rpsy_{161}$	$rpsyu_{161}$
$mm_1/dd_7/yyyy_1$	$rpsy_{171}$	$rpsyu_{171}$
.	.	.
.	.	.
.	.	.
$mm_2/dd_1/yyyy_1$	$rpsy_{211}$	$rpsyu_{211}$
$mm_2/dd_2/yyyy_1$	$rpsy_{221}$	$rpsyu_{221}$
.	.	.
.	.	.
.	.	.
$mm_1/dd_1/yyyy_2$	$rpsy_{112}$	$rpsyu_{112}$
.	.	.
.	.	.
.	.	.
$mm_p/dd_q/yyyy_r$	$rpsy_{pqr}$	$rpsyu_{pqr}$

Site information for all selected wells

ID	Lat	Long	Depth (m)
j_1	x_1	y_1	d_1
j_2	x_2	y_2	d_2
j_3	x_3	y_3	d_3
j_4	x_4	y_4	d_4
j_5	x_5	y_5	d_5
j_6	x_6	y_6	d_6
j_7	x_7	y_7	d_7
.			
.			
.			
j_{81}	x_{81}	y_{81}	d_{81}

Figure S10: File format of the RpSy and RpSyu dataset.

References

Bhanja, S. N., Mukherjee, A., Rangarajan, R., Scanlon, B. R., Malakar, P., & Verma, S. (2019). Long-term groundwater recharge rates across India by in situ measurements. *Hydrology and Earth System Sciences*, *23*(2). https://doi.org/10.5194/hess-23-711-2019

Brooks, R., & Corey, A. (1964). Hydraulic properties of porous media. *Hydrology Papers, Colorado State University*, *3* (March).

Chaney, N. W., Minasny, B., Herman, J. D., Nauman, T. W., Brungard, C. W., Morgan, C. L. S., McBratney, A. B., Wood, E. F., & Yimam, Y. (2019). POLARIS Soil Properties: 30-m Probabilistic Maps of Soil Properties Over the Contiguous United States. *Water Resources Research*, *55*(4). https://doi.org/10.1029/2018WR022797

Crosbie, R. S., Binning, P., & Kalma, J. D. (2005). A time series approach to inferring groundwater recharge using the water table fluctuation method. *Water Resources Research*, *41*(1). https://doi.org/10.1029/2004WR003077

Fan, J., Oestergaard, K. T., Guyot, A., & Lockington, D. A. (2014). Estimating groundwater recharge and evapotranspiration from water table fluctuations under three vegetation covers in a coastal sandy aquifer of subtropical Australia. *Journal of Hydrology*, *519*(PA). https://doi.org/10.1016/j.jhydrol.2014.08.039

Jasechko, S., Seybold, H., Perrone, D., Fan, Y., & Kirchner, J. W. (2021). Widespread potential loss of streamflow into underlying aquifers across the USA. *Nature*, *591*(7850). https://doi.org/10.1038/s41586-021-03311-x

McKay, L., Bondelid, T., Dewald, T., Johnston, J., Moore, R., & Rea, A. (2012). *NHDPlus Version 2: User Guide*.

Siva Prasad, Y., & Venkateswara Rao, B. (2018). Groundwater recharge estimation studies in a khondalitic terrain of India. *Applied Water Science*, *8*(4). https://doi.org/10.1007/s13201-018-0738-2

U.S. Geological Survey. (2019). *3D Elevation Program 1-Meter Resolution Digital Elevation Model*.

van Genuchten, M. Th. (1980). A Closed-form Equation for Predicting the Hydraulic Conductivity of Unsaturated Soils. *Soil Science Society of America Journal*, *44*(5). https://doi.org/10.2136/sssaj1980.03615995004400050002x

Wieczorek, M. E., Jackson, S. E., & Schwarz, G. E. (2019). *Select Attributes for NHDPlus Version 2.1 Reach Catchments and Modified Network Routed Upstream Watersheds for the Conterminous United States USGS data release v. 2.0*. USGS.

Yin, L., Hu, G., Huang, J., Wen, D., Dong, J., Wang, X., & Li, H. (2011). Groundwater-recharge estimation in the Ordos Plateau, China: Comparison of methods. *Hydrogeology Journal*, *19*(8). https://doi.org/10.1007/s10040-011-0777-3

Zhang, Z., Wang, W., Gong, C., Zhao, M., Wang, Z., & Ma, H. (2021). Effects of non-isothermal flow on groundwater recharge in a semi-arid region. *Hydrogeology Journal*, *29*(2). https://doi.org/10.1007/s10040-020-02217-8